Optim Eng (2016) 17:77–103
DOI 10.1007/s11081-016-9308-3

A hybrid extended pattern search/genetic algorithm for multi-stage wind farm optimization

Bryony DuPont[1] · **Jonathan Cagan**[2]

Received: 29 November 2014 / Revised: 17 August 2015 / Accepted: 21 December 2015 /
Published online: 14 January 2016

Abstract This purpose of this work is to explore means of optimizing multi-stage wind farms using two derivative-free optimization methods: a hybrid Extended Pattern Search/Genetic Algorithm (capitalizing on the benefits of each), and a multi-objective Extended Pattern Search. Large onshore wind farms are often installed in discrete phases, with smaller sub-farms being installed and becoming operational in succession, creating the completed large wind farm in a piece-wise fashion over multiple years. Multi-stage wind farms present a complex and relevant optimization challenge in that in addition to accounting for the site-specific objectives of a wind farm (such as power development and profit), optimization of both the discrete sub-farms and the completed farm must be jointly considered. Two different problem formulations are explored: the first uses the optimal layout of a complete farm and then systematically "removes" turbines to create smaller sub-farms; the second uses a weighted multi-objective optimization over sequential, adjacent land that concurrently optimizes each sub-farm and the complete farm. For both problem formulations, two wind test cases are considered for both a square and a rectangular field: a constant wind speed from a predominant wind direction, and a multidirectional test case with three wind speeds and a defined probability of occurrence for each. The exploration of these resulting layouts indicates the value of the advanced multi-objective EPS and the hybrid EPS/GA, and gives insight into how to approach

This paper is an extended version of a conference paper in ASME proceedings DuPont and Cagan (2013).

✉ Bryony DuPont
bryony.dupont@oregonstate.edu

Jonathan Cagan
cagan@cmu.edu

[1] Oregon State University, Rogers Hall 216, Corvallis, OR 97331, USA

[2] Carnegie Mellon University, Scaife Hall 5000 Forbes Ave, Pittsburgh, PA 15232, USA

optimizing both completed wind farms and sub-farm stages. The behavior exhibited in these tests cases suggests strategies that can be employed by wind farm developers to facilitate predictable, optimal performance of multi-stage wind farms throughout their useful life.

Keywords Extended pattern search · Genetic algorithm · Wind farm optimization

1 Introduction

Work in the computational optimization of wind farm layouts has been explored for many years, though significant advances have been made recently due to increasing computational capability and interest. The driving force influencing wind farm layout optimization is the fact that turbines that are placed in close proximity can experience power development deficits due to the decrease in wind speed caused by the rotating blades of neighboring (upstream) turbines. While the addition of more turbines to a site will generally allow for the generation of more power, one must consider potential array losses (the reduction of power development) in determining the local positioning of each turbine (Manwell et al. 2009).

Many new onshore wind farms in the Unites States include a large number of turbines, such as the 390-turbine 1020 MW Alta Wind Energy Center in California (Terra-Gen Power 2015), the 627-turbine 781.5 MW Roscoe Wind Farm in Texas E.ON (Climate and Renewables 2015), and the 421-turbine 735.5 MW Horse Hollow Wind Energy Center in Texas (Next Era Energy Resources 2006). Each of these was built in multiple stages, that is, preliminary smaller sub-farms were installed and integrated into the electricity grid, and subsequent sub-farms were built; the combination of these sub-farms leads to the completed large farm. Additional stages tend to be on adjacent plots of land, and often exhibit the placement of turbines in straight lines to benefit from a predominant wind direction (such as the 222 MW, three-stage Stateline Wind Project in Oregon (Oregon DOE 2010)). This presents an intriguing and complex layout problem from an engineering optimization perspective—the optimal layout for the completed farm is not likely to be the aggregate of the optimal layouts of the discrete sub-farms. However, it is uncommon for large multi-stage wind farms to be optimized *a priori*.

The complexity of the multi-stage wind farm problem stems from the extensive modeling used to represent cost, wind farm aerodynamic interactions, and power development; all of these are considered iteratively as turbine geometry and locations change throughout the search, and each of these searches happen concurrently for individual wind farm stages. The problem formulations included in this work require both continuous and discrete variable selection, further suggesting the application of derivative-free optimization (DFO) methods such as the EPS/GA. It should also be noted that both the development of optimization methods described next, and the application of these to the multi-stage wind farm problem, are the fundamental research being explored; therefore the use of available DFO solvers, such as NOMAD (Abramson et al. 2009; Le Digabel 2011) and DFL (Di Pillo et al. 2015), are not considered.

Two different optimization methods (the hybrid EPS/GA and a multi-objective EPS) were developed to accommodate the two problem formulations presented in this work. Both algorithms advance the capability of an established EPS algorithm for wind farm optimization (DuPont and Cagan 2010, 2012; DuPont et al. 2012, 2016). First, the "Full-Farm" optimization uses the hybrid EPS/GA to create an optimal layout of a complete farm and then systematically "removes" turbines to create smaller sub-farms. The second method, the weighted multi-objective EPS over sequential, adjacent land, consists of each stage being assigned to adjacent plots of land, concurrently optimizing each sub-farm and the complete farm. Test cases are performed on two different farm configurations that are commonly seen in the United States—a square field and a rectangular field aligned perpendicular to the predominant wind direction.

The exploration of the resulting layouts indicates the value of full-farm optimization (in addition to optimization of the individual stages) and informs how to optimize sub-farm stages. The behavior exhibited in these tests cases gives insight that can be employed by wind farm developers to ensure that multi-stage wind farms perform optimally throughout their completion. That is, the full-farm optimization seeks to explore an optimization taking place *over time*; the time-relevant parameters of the cost model allow for the addition of stages over multiple years. Moreover, we want to understand how the hybrid EPS/GA works as applied to large-scale systems optimization problems that necessitate traversing a large search tree to solve, and to theorize potential alternative test problems for this algorithm. For example, large systems that require concurrent layout of subassemblies, such as commercial airliners or large-scale electricity supply systems, may be suitable potential applications for the hybrid EPS/GA.

2 Previous literature

2.1 Wind farm optimization

Of the varying computational algorithms applied to wind farm layout optimization, Genetic Algorithm (GA) approaches have been the most popular. The first of these, by Mosetti et al. (1994), established the test scenario that has been repeatedly employed for comparison purposes. This test case is a square 2 km $\times$ 2 km field, depicting an aerial view of turbines on a 2-D discretized solution space. Mosetti et al.'s GA used an objective function that maximized the power development of the farm while minimizing an estimation of the normalized cost, and employed wake modeling developed by Jensen (1983) to determine the effective wind speed at each turbine. Grady et al. (2005) introduced a GA that improved upon Mosetti et al.'s method by utilizing advanced computational resources. Though these researchers were on the forefront of heuristic optimization as applied to wind farm layout, recent research has expanded upon the performance of these preliminary works.

Multiple reports by Elkinton et al. (2005, 2006) suggest that Genetic Algorithms are best suited for offshore wind optimization. Wan et al. (2009) utilized the same discretized solution space as previous researchers, but applied

more accurate modeling of power. Wang et al. used grid-placement techniques in conjunction with a GA (2009b), and employed non-linear wake expansion to estimate the effects of wakes (2009a). Huang used a distributed GA (DGA), which divided large populations into smaller populations for computational efficiency (2007), and later combined this DGA with a gradient search method to produce more optimal layouts (2009). Sisbot et al. (2009) applied a multi-objective GA to a realistic potential wind site, using advanced cost modeling, while Emami and Noghreh (2010) also used a weighted multi-objective GA to explore the trade-off between wind farm power development and cost. Rasuo and Bengin (2010) explored the application of a GA to wind farms on varied terrain, which captured real-world topographical challenges in wind farm micrositing. These GA approaches have integrated means of handling some real-world wind farm optimization issues, but many of these utilize a coarsely discretized solution space, reducing the algorithm's ability to effectively pack the farm area with turbines (DuPont and Cagan 2012).

In addition to genetic algorithms, multiple other methods have been used to solve the wind farm layout optimization problem. Aytun Ozturk and Norman (2004) used a set of heuristic rules to place turbines, while Bilbao and Alba (2009) employed a simulated annealing algorithm. Mustakerov and Borissova (2010) developed a mixed-integer nonlinear discrete combinatorial optimization algorithm that employed both a square and rectangular solutions space, which influenced the use of those shapes in the solutions spaces of the current work. Wan et al. (2010) expanded on their previous GA approach by creating a particle swarm optimization (PSO) approach. More recent work includes offshore wind farm layout optimization using a Coral Reefs optimization method (Salcedo-Sanz et al. 2014), and an improved Discrete Development Model—representative of cellular division—for onshore wind farm layout optimization (Wilson et al. 2014). The methodology on which the current work is based, an extended pattern search, has also been successfully applied to wind farm layout optimization and has incorporated multiple advances in modeling that enable the development of more real-world applicable wind farm layouts (DuPont and Cagan 2012; DuPont et al. 2012).

There are several recent works that seek to expand on the capability of various algorithms such that state-of-the-art modeling of cost, wake interaction, and power are incorporated into the optimization. Zhang et al. (2010) created a cost surface to more accurately estimate the costs associated with wind farm development. Chowdhury et al. (2010) established a framework for the selection of turbines with varying rotor radii, and DuPont et al. (2012) expanded the capability of their EPS algorithm to select both turbine hub heights and rotor radii. Benatiallah and Dakyo (2010) used actual long-term wind data as an input to their genetic algorithm for wind farm layout. Chen and Macdonald (2011) explored the implications of landowner decisions on resulting farm layouts. Kusiak and Zheng (2010) used preliminary data mining in conjunction with a GA to determine the optimal control settings for a proposed farm. More recent work by Chowdhury et al. (2013) used a kernel density estimation to better model multi-modal wind data. These advances suggest that it is not only the choice and development of the optimization algorithm

itself, but also the advances in how wind farm optimization is modeled that will lead to robust and thoroughly tested proposed layouts that perform as predicted.

2.2 Derivative-free optimization of complex systems

The optimization of complex systems often includes nonlinear and/or non convex objective functions and models. The large onshore multi-stage wind farms problem formulation presented in this work is no exception. These types of systems require optimization methods that are functionally designed to accommodate these nonlinearities, to help traverse a search space that includes a plethora of local minima, and preclude the calculation of derivatives in the objective formulation. Such Derivative-Free Optimization (DFO) (Conn et al. 2008) methods were first formalized by Hooke and Jeeves (1961), who introduced direct search methods that, as an alternative to calculating derivatives (such as steepest-descent), employed "sequential examination of trial solutions", and greediness that facilitated search convergence. The pattern search (PS) method that serves as the foundation of the algorithms explored in this work is a type of direct search (Torczon 1997).

Multiple recent works have explored the development of DFO algorithms and their application to engineering test problems. Fowler et al. (2008) applied DFO methods specifically designed for constrained engineered systems optimization problems (specifically, groundwater supply and hydraulic capture) and showed variation between different algorithms, such as APPS, NSGA-II, and NOMAD. Audet and Dennis (2006, Audet et al. 2008a) created the Mesh Adaptive Direct Search (MADS) algorithm, which is a generalization of a pattern search, and explored both single- and multi-objective formulations (Audet et al. 2008b) to determine the algorithm's efficacy in determining Pareto optimal points.

Most similar to the current work, Vaz and Vicente (2007) developed a hybrid algorithm—the combination of multiple DFO methods, similar to the EPS/GA presented in this work—that combined a pattern search algorithm with a particle swarm optimization (lPSO). These hybrid methods are designed to capitalize on the benefits of each algorithm; in the case of the PS/PSO hybrid method, classical optimization problems from literature were solved by employing a sub-level PSO that identified neighborhoods of global minimizers, and the deterministic PS performed the overarching traversal of the search space.

In keeping with the current trend to advance both modeling and algorithm capability, the current work establishes the means to develop wind farms in stages, such that the best layout (in terms of minimizing the objective function) is considered during both sub-farm and complete farm implementation. The EPS algorithm (DuPont et al. 2012) is used as the basis for the optimization, as it is designed to select both turbine placement and geometry, account for variation in atmospheric stability conditions and wind shear profile shape, incorporate the effects of partial wake interaction. This EPS algorithm has previously developed superior layouts than comparable algorithms on traditional test cases (DuPont et al. 2012; DuPont and Cagan 2013).

3 EPS and hybrid EPS/GA methodology

Two optimization methods are presented in this work—a multi-objective EPS and a hybrid EPS/GA Algorithm. Psuedocode depicting the (A) EPS and the (B) GA are shown in Figs. 1 and 2, respectively. Extended pattern search is a derivative-free algorithm that is based on a traditionally deterministic pattern search (PS) algorithm. A traditional pattern search (PS) works as follows: an element in the continuous search space traverses through a user-defined set of pattern directions (in this case, the four cardinal directions in (x,y) space) at a given step size, testing the objective function evaluation at each potential move. Potential moves are screened such that constraints are not violated; in this case, turbines cannot be moved outside the solution space, and cannot be moved within a minimum distance—5 rotor diameters—of any other turbine. A move is only selected if it does not violate the constraints, and it benefits the global evaluation; if no potential moves are chosen at a given step size, the step size is reduced and the search is repeated. The EPS stopping criterion is met when the search reaches a minimum user-defined step size.

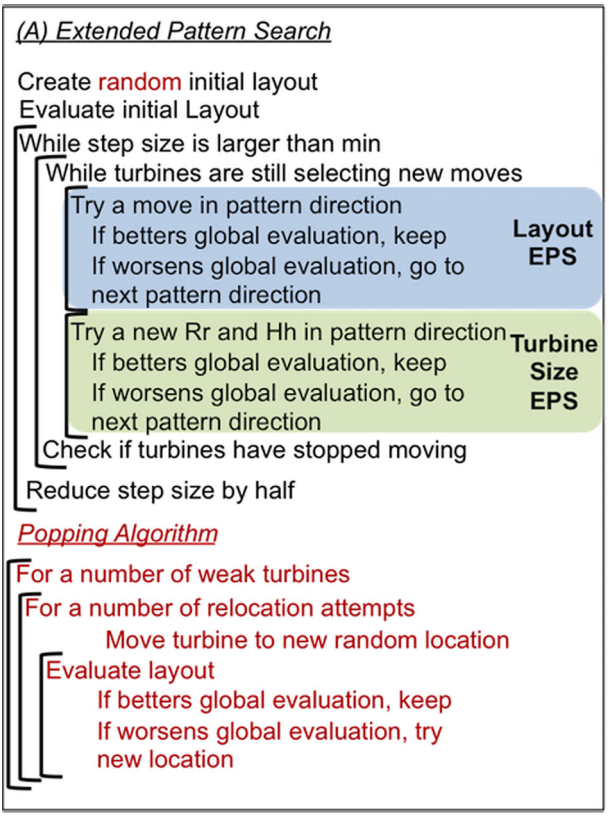

Fig. 1 **a** Pseudocode for extended pattern search. Hh and Rr represent hub height and rotor radius, respectively

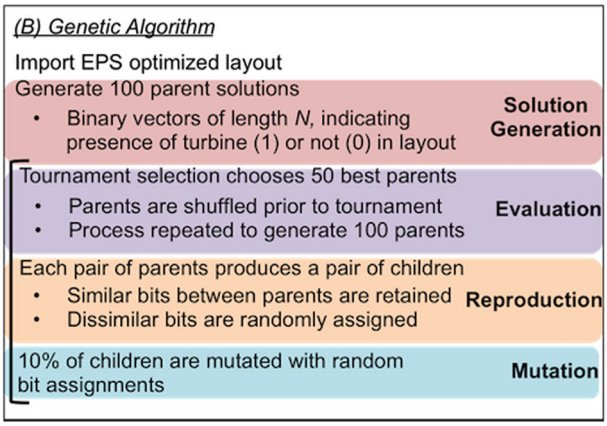

Fig. 2 **b** Pseudocode for genetic algorithm

The deterministic behavior of the EPS leads to certain solution finding (given the objective function has searchable optima), but as with other heuristic optimization approaches, global optimality is not guaranteed.

The derivative-free EPS algorithm upon which both methods are based improves upon the traditional deterministic pattern search (PS) algorithm in that it includes stochastic elements (called "extensions") to facilitate escaping inferior local optima. The EPS generally requires fewer function evaluations than comparable heuristic algorithms, such as simulated annealing algorithms (Cagan et al. 2000), and inherently handles continuous solution spaces. Driven by its successful application to other complex layout problems (Yin and Cagan 2000), the EPS algorithm has previously been applied to wind farm layout optimization, producing results superior to comparable heuristic optimization algorithms (DuPont and Cagan 2012). To enable the search to escape local optima, three stochastic *extensions* are employed in this work, hence *Extended* Pattern Search (EPS): (1) an initial random layout removes any bias that may come about by a user-defined initial placement, (2) the search order through which the algorithm determines what turbine to move is randomized such that no turbine's movement is favored, and (3) a "popping" algorithm that selects poorly-performing turbines based on power development attempts to relocate these turbines to random locations, allowing the move only if it benefits the global evaluation (DuPont and Cagan 2012). In Fig. 1, these extensions are indicated in red font.

The foundational EPS algorithm for turbine layout also includes two concurrent sub-level EPS algorithms that select both turbine hub height and rotor radius, constraining the relationship between the two such that infeasible designs are not considered (DuPont et al. 2012). This enables the search to not only move turbines such that they avoid being placed in the wakes of upstream turbines, but to also select turbine geometry that can help avoid wake interaction and maximize individual turbine power development. The layout EPS is indicated by the blue box in Figure 1, and the hub height and rotor radius EPS is indicated by the green box.

The limiting factor used to determine the size of wind farm stages is the number of turbines, which is indicative of some of the limiting factors that might be seen in actual wind farm development, such as limited up-front capital. Though multi-stage wind farms tend to be very large, to reduce computational expense the current work explores a representative test case of a completed wind farm of 40 turbines, with stages being added in increments of 10.

3.1 Full-farm optimization with hybrid EPS/GA

The hybrid EPS/GA is designed for application to multi-modal problems that require efficiently searching a very large, continuous search space. The multi-stage wind farm optimization problem can be formalized to use this particular algorithm, as the selection of turbine locations and geometry is 3-D multi-modal, and the use of multiple stages significantly increases the size of the solution space—in addition to determining turbine location and geometry, the algorithm must also determine the relative timing of when the turbine is installed. In this problem formulation, the overall space is optimized using the EPS algorithm depicted in Fig. 1, then the GA determines which turbines will be installed in each stage (shown in Fig. 2). For the multi-stage wind farm optimization problem, this corresponds to a focus on the optimization of the completed farm, hence the "Full-Farm" descriptor. The full farm (both a square and rectangular layout, as depicted in Fig. 3) is optimized using the EPS algorithm. The GA "removes" turbines from the full-farm layout to meet the specified number of turbines associated with the development of each sub-farm. The staging order is then reversed, such that the last turbines to be removed constitute the first sub-farm, as shown in Fig. 4.

This approach intentionally differs from the way multi-stage farms are traditionally developed, in that instead of adding new independent stages of turbines to adjacent land, a large initial solution space is used, and turbines are added throughout the entire space during every additional stage. The optimization of completed wind farms has yet to be approached in this manner, and exploration of this method implicates potential superiority over the traditional adjacent-land multi-stage wind farm approach. As this process, which involves the creation of a large tree structure, is computationally expensive—the equivalent expense of running the EPS 40 times—the sub-level GA approach is an efficient way of traversing this tree

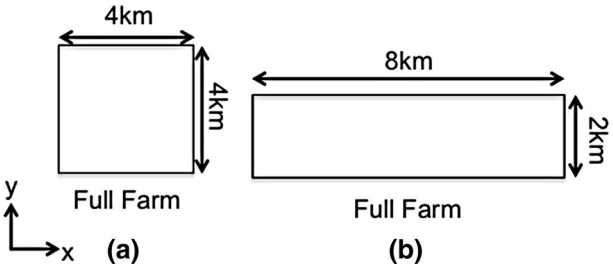

Fig. 3 "Full-Farm Optimization": **a** 4 km × 4 km square field, **b** 2 km × 8 km rectangular field

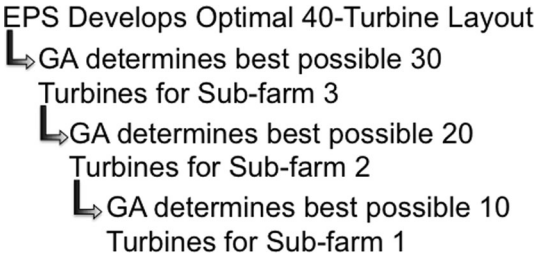

Fig. 4 Hierarchy for full-farm hybrid Eps/Ga approach

structure. Once the EPS for both layout and turbine size is is completed for 40 turbines (as shown in Fig. 1), each turbine will be removed individually and the global objective will be evaluated for each removal (shown in GA pseudocode in Fig. 2). The turbine with the least impact on the global objective is removed, and the search repeats, as shown in Fig. 4.

The GA used to search the solution tree is based on the micro-GA work of Senecal (2000), where the "micro" designation implies there are a relatively small number of parent strings. With the final farm positions and turbine geometries selected by the EPS, the GA is employed to determine which of the 40 turbines will be included at each stage of the farm's development. The GA consists of binary parent strings that indicate whether or not a turbine exists in the optimal EPS-derived layout. For the full layout of 40 turbines, a set number (in this case, a stage of 10) of turbines are removed from the parent strings, such that the solution includes just the number of turbines for the next-smallest-sized sub-farm. The objective evaluation between parents compares the potential profit (as given in Eq. (7)) for a farm whose included turbines are defined by the parent string (indicated by the purple box in Fig. 2). Parents are paired and reproduced to create a pair of children; this reproduction occurs by propagating similar bits between parents and randomly assigning dissimilar bits (orange box, Fig. 2). To enable the GA to escape local optima, mutation is included (blue box, Fig. 2). The evaluation, reproduction, and mutation sections are repeated until the stopping criteria is met; in this case, this is when the top 80% of children are identical to their parents, all of which are identical to each other. After the sub-farm of 30 is generated, the process repeats to develop the sub-farm of 20, and so on. The GA was performed ten times using 100 parent strings, and resulted to the same layout every trial.

3.2 Weighted multi-objective EPS over sequential, adjacent land

A second approach to wind farm layout optimization in stages is the use of a weighted multi-objective EPS algorithm. This algorithm is applied to individual layout fields, and their weighted sum constitutes the global objective evaluation for all of the fields together. In this test case, each wind farm stage is installed on separate land (divided into sub-farms as depicted in Fig. 5). The weighted multi-objective formulation consists of both the individual evaluations of each sub-farm and the evaluation of the full farm. Each of these objectives has an associated user-defined weighting factor that determines the percent at which each evaluation will

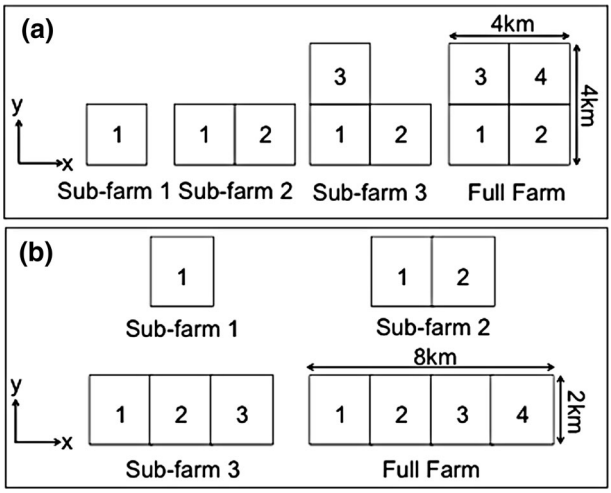

Fig. 5 Multi-objective optimization **a** 4 km × 4 km square field, **b** 2 km × 8 km rectangular field

contribute to the global objective. The weighted sum methodology, as formulated in Eq. (1), builds on previous work in multi-objective wind farm optimization (Kusiak and Zheng 2010; Samorani 2010). It should be noted that while there are potential concerns with the use of weighted sums in multi-objective optimization (this method may not result in the development of a realistic Pareto optimal set (Messac 1996)), the use of this method herein is exploratory; the weighted sum method allows for a clear impact analysis of the trade-off between the objective function evaluation of individual wind farm stages and the objective function evaluation of the full farm.

$$\begin{aligned} Objective_{Global} = {} & w_1 Objective_{SubFarm1} + w_2 Objective_{SubFarm2} \\ & + w_3 Objective_{SubFarm3} + w_4 Objective_{FullFarm} \end{aligned} \tag{1}$$

The weighted multi-objective EPS seeks to explore the trade-off between optimizing the individual layout fields and the overall complete field. For the multi-stage optimization problem, the individual fields are sub-farms (which are operational years prior to the completion of the farm) and the complete field is the full-farm layout. As a preliminary exploration of the trade-off between sub-farm and full-farm objectives, each weighting factor is initialized to 25%, meaning that each sub-farm has the same weighting. Each of the four stages is restricted to contain only 10 turbines, which constrains the layout to represent building stages on adjacent land.

4 Problem formulation

Two test cases that are commonly used in previous wind farm optimization literature are considered for comparison purposes (DuPont and Cagan 2012; Grady et al. 2005; Mosetti et al. 1994). The first case is constant, unidirectional wind

(shown in Fig. 6a), and the second is multidirectional, varying wind speeds, as shown in Fig. 6b. For the multidirectional test case, each wind direction and wind speed has an associated fraction of occurrence, as shown in Fig. 7. The unidirectional case, while simplified, is representative of a wind farm for which a snapshot wind condition is considered, or those farm locations that have a consistently dominating wind direction. The multidirectional case has a prominent directional quadrant from which the wind is most likely to blow, representing likely wind conditions for large onshore wind farms. For both problem formulations, square and rectangular solution spaces are employed.

5 Modeling

5.1 Wake model and partial wake interaction

The flow behind rotating turbine blades is complex and difficult to capture without incurring significant computational cost, so the need to analytically model downstream airflow is paramount in highly iterative algorithms like EPS. The hybrid EPS/GA and the multi-objective EPS employed in this work utilize a 3-D extrapolation of the PARK wake model to estimate the effect that a wind turbine has on the air flow directly downstream of its rotor (Jensen 1983). This wake is assumed to be conical in shape (as shown in Fig. 8) wherein the wind speed is significantly reduced just behind the rotor but continually gains speed and asymptotically approaches the ambient wind speed as the wake traverses downstream distance. Mathematically, both the width of the downstream wake and the wind speed deficit are proportional to the distance downstream from the rotor, as stated in the momentum balance given in Eq. (2):

$$\pi r_r^2 v + \pi(r_1^2 - r_r^2)U_0 = \pi r_1^2 U \tag{2}$$

In Eq. (2), U_0 is the ambient wind speed colorgreen (the speed of the wind approaching the farm), r_r is the radius of the turbine rotor, r_1 is the radial width of the wake at distance y downstream from the turbine, v is the velocity directly behind

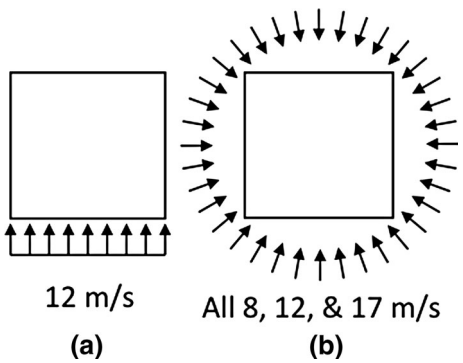

Fig. 6 **a** Unidirectional, constant wind speed case, **a** Multidirectional, varying wind speed case

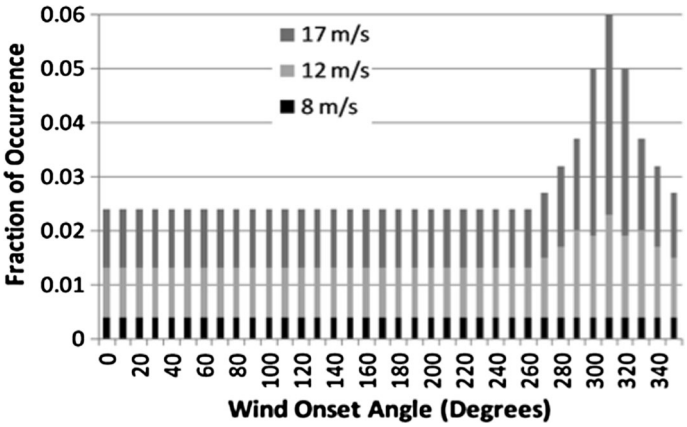

Fig. 7 Probability of occurrence for wind direction and wind speed, multidirectional case

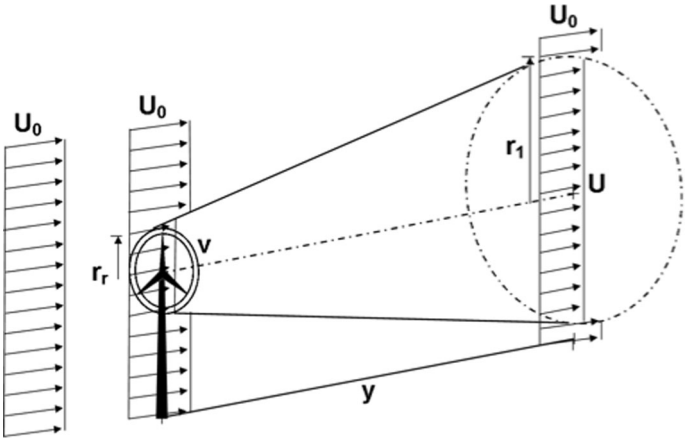

Fig. 8 Depiction of frustum-shaped 3-D Wake

the turbine (approximately 1/3 of the ambient wind speed), and U is the wind speed within the wake at distance downstream. U is a reduced from the ambient wind speed U_0 (as the rotor harvests momentum) and is abstracted to be constant across the cross-section of the wake. The formula for U, the downstream wind speed within the wake, is given by:

$$U = U_0\left(1 - \frac{2}{3}\left(\frac{r_r}{r_r + ky}\right)\right) \tag{3}$$

A turbine that is placed such that it does not incur any wake effects from upstream turbines has an effective wind speed equivalent to the unobstructed ambient wind speed approaching the farm. To determine the effective wind speed for any turbine that lies within a single wake, Eq. (3) is used, where k is the wake decay for the

neutral atmospheric stability case. To calculate the effective wind speed for a turbine placed in multiple wakes, the individual kinetic energy losses caused by each of the n wakes must be summed using Eq. (4):

$$U = U_0\left(1 - \sqrt{\sum_{i=1}^{n}\left(1 - \frac{U_i}{U_0}\right)^2}\right) \tag{4}$$

At each iteration, a rectangular neighborhood in (x, y) is used to preliminarily determine which turbines have wake interactions, using Eq. (5) to determine the width of the wake at a given distance:

$$r_1 = r_r + ky \tag{5}$$

Using these rectangular neighborhoods, each rotor's frustum-shaped wake is established to determine the percentage of the rotor swept area of downstream turbines that lie within that wake. Three distinct partial wake interaction scenarios are considered (DuPont et al. 2012). The first is a turbine rotor that is partially located within the wake of one upstream turbine, or two upstream turbines whose wakes do not overlap across the rotor swept area, such that each percentage of overlap can be calculated individually. The second is the case of multiple wakes that overlap across a turbine's rotor swept area, which necessitates a discretization of the rotor swept area in order to estimate the combinatory effects of the overlapping portions of the wakes. The third scenario, which is unlikely due to wake expansion during propagation, is when the entire cross-section of a wake lies within the rotor swept area of a downstream turbine; the percentage of overlap in this case can be calculated directly.

The use of the PARK wake model is imperative to ensure the efficient computational time of the EPS algorithm, but it does simplify the complex wake behavior created by rotating turbine blades. Primarily, the wind speed within a wake is considered constant across the cross-section, and exhibits binary behavior at the wake boundary that would be more accurately represented by a wind speed gradient (Katic et al. 1986). The model also lacks the capability to capture the complex wake behavior directly behind a rotor, though the minimum-distance requirement between turbines is large enough to ensure that turbines are not placed in these difficult portions of the wakes.

In addition, the EPS algorithm incorporates local information (air density and the height of the rotor from the ground) about the potential farm site's atmospheric stability conditions to more accurately predict the power development of the farm. In the atmospheric boundary layer—the region of air closest to the earth's surface—variation in temperature, local wind direction, humidity, air density, and other parameters often occur due to changes in atmospheric stability. For simplification, the current work uses site-averaged neutral atmospheric condition parameters derived from the Lamar Low Level Jet (LLLJP) data (Kelley et al. 2004). Further information about the accounting for atmospheric stability in wind farm optimization can be found in previous work by DuPont et al. (2012).

5.2 Power modeling

An estimation of the power development of a single turbine is given in Eq. (6) (Manwell et al. 2009):

$$P = \frac{1}{2}\rho A U^3 C_p \tag{6}$$

where ρ is the density of air (considered constant at 1.225 kg/m^3), A is the cross-sectional area swept by the rotor blades, U is the effective wind speed (the wind speed directly in front of the turbine's rotor, and C_p is the power coefficient. Additionally, to mimic the power curves of commercially available turbines, a rated wind speed of 11.5 m/s is enforced, such that at wind speeds higher than the rated wind speed, a turbine will only produce the amount of power it would at 11.5 m/s. The turbine will not produce power at wind speeds below the cut-in speed of 3 m/s. The total power output of the farm is considered to be the sum of the individual power developments of each turbine.

5.3 Cost modeling

The National Renewable Energy Laboratory's Wind Cost and Scaling Model (Fingersh et al. 2006) was used to create a realistic prediction of the costs associated with installing a wind farm. The total estimation of cost contains many factors, such as the land lease costs for the farm site, the materials and manufacturing costs for turbine production, and the operation and maintenance costs of the farm. To facilitate wind farm developers and researchers, the NREL cost model is integrated into a freely-available spreadsheet, called the Jobs and Economic Development Impact (JEDI) model for wind (NREL) that was used to develop the cost surface employed in this work. A matrix of feasible turbine geometries was developed along with the resulting predicted power development of each combination of hub height and rotor radius. This matrix was then used as an input to the JEDI spreadsheet, which created an estimation of cost based on hub height and rotor radius. The analytical cost model used in this work is developed from this black box model, simulating the complex and interrelated aspects of wind farm cost but passing only the turbine geometry as input. The cost surface for neutral stability conditions is pictured in Fig. 9.

The cost as a function of hub height and rotor radius for neutral stability conditions is given in Eq. (7):

$$\begin{aligned} Cost(h,r) = {} & (2.45e+06) - (2.161e+05)r + (1.203e+04)h \\ & + 6039r^2 + 2455rh - 1.61.2h^2 \end{aligned} \tag{7}$$

5.4 Objective function

The objective function used for evaluation in both the hybrid EPS/GA and the multi-objective EPS algorithms is that of profit maximization over a set farm lifetime. To

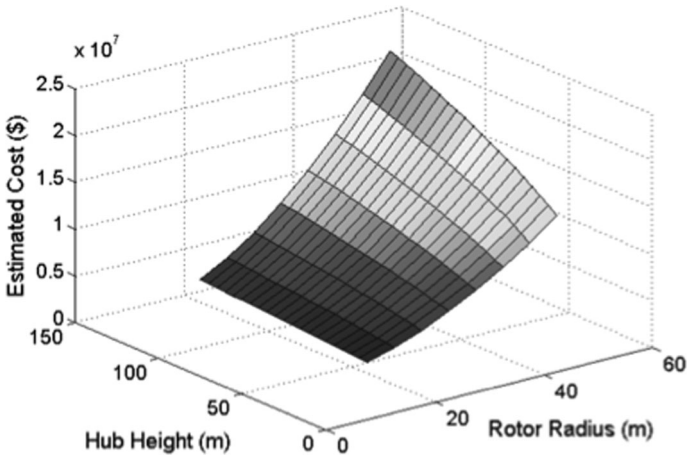

Fig. 9 Cost surface developed from NREL Jedi Spreadsheet (Neutral Stability Conditions)

conform to traditional negative null form, the objective function considered here is the minimization of negative profit. Once the total power development of the farm and the total cost (the sum of the individual turbine costs) are calculated, the objective function can be evaluated:

$$Objective = Cost_{Project} + (Cost_{O\&M}\ t) - (Energy_{Yearly}\ C_F\ t\ COE) \tag{8}$$

$$Cost_{O\&M} = 0.007\ Energy_{Yearly}\ C_F\ t\ COE \tag{9}$$

where C_F is the capacity factor, and COE is the cost of energy—the price at which a farm owner may sell the energy their farm develops, in $\$/kWh$, and t is the life of the farm in years. $Cost_{Project}$ is the cost that is estimated using the cost surface formula in Eq. (7). $Cost_{O\&M}$ is the annual operations and maintenance cost of the farm in $\$/year$, and is given by Eq. (9) (Fingersh et al. 2006).

The life of each turbine is considered to be 20 years. Future work will consider the life of each sub-farm in addition to the life of the farm as a whole, and how having earlier turbines that have longer relative lives affects the optimization.

6 Results

Results are presented for (A) the full-farm hybrid EPS/GA case, and (B) the multi-objective EPS case. Both methodologies explore a square and a rectangular layout, and two wind cases: constant, unidirectional wind (constant in the +y direction at 10 m/s), and multidirectional, varying wind speeds (8, 12, and 17 m/s). The turbine geometries are indicated using symbols and colors representing hub height and rotor radius, as shown in Figure 10. A minimum distance requirement is enforced to ensure that turbines are not placed too close together. The results for the full-farm optimization scenario are shown in increments of ten turbines, such

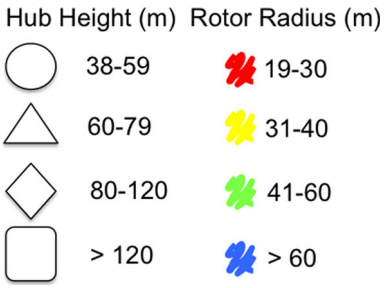

Fig. 10 Key for turbine geometry

that the first result for a given set of conditions is the first ten turbines of the proposed farm, constituting the first stage. The following figure shows then next ten turbines (the second stage), added to the first stage to create a new sub-farm. This cumulative process repeats until the complete farm, consisting of 40 turbines, is shown.

6.1 Unidirectional case

6.1.1 Full-farm optimization with hybrid EPS/GA, unidirectional case

The full-farm optimization starts with an EPS-derived 40-turbine optimal layout, then proceeds to "remove" turbines using a GA, in batches of ten, creating three smaller sub-farms (containing 30, then 20, then 10 turbines each). In theory, a wind farm developer would start with the smallest farm (in this case, 10 turbines), and add turbines in the prescribed stages until the full farm is complete. The numerical results for each square sub-farm are compiled in Table 1, with the square sub-farm layouts given in Fig. 11. The numerical results for the rectangular field are given in Table 2, with the rectangular sub-farm layouts given in Fig. 12.

6.1.2 Weighted multi-objective EPS over sequential, adjacent land, unidirectional case

The weighted multi-objective EPS over sequential, adjacent land approach constrains the number of turbines placed in each subsequent stage, representing a limit on the capital available for each stage of the proposed wind farm. A wind farm

Table 1 Unidirectional full-farm hybrid EPs/GA results, square field

N	Objective	Power (MW)	Avg. hub height (m)	Avg. rotor radius (m)
40	−1.23E+08	150	111.31	52.46
30	−1.11E+08	139	126.69	59.85
20	−7.94E+07	109	134.77	65.85
10	−4.42E+07	55.9	134.77	66.35

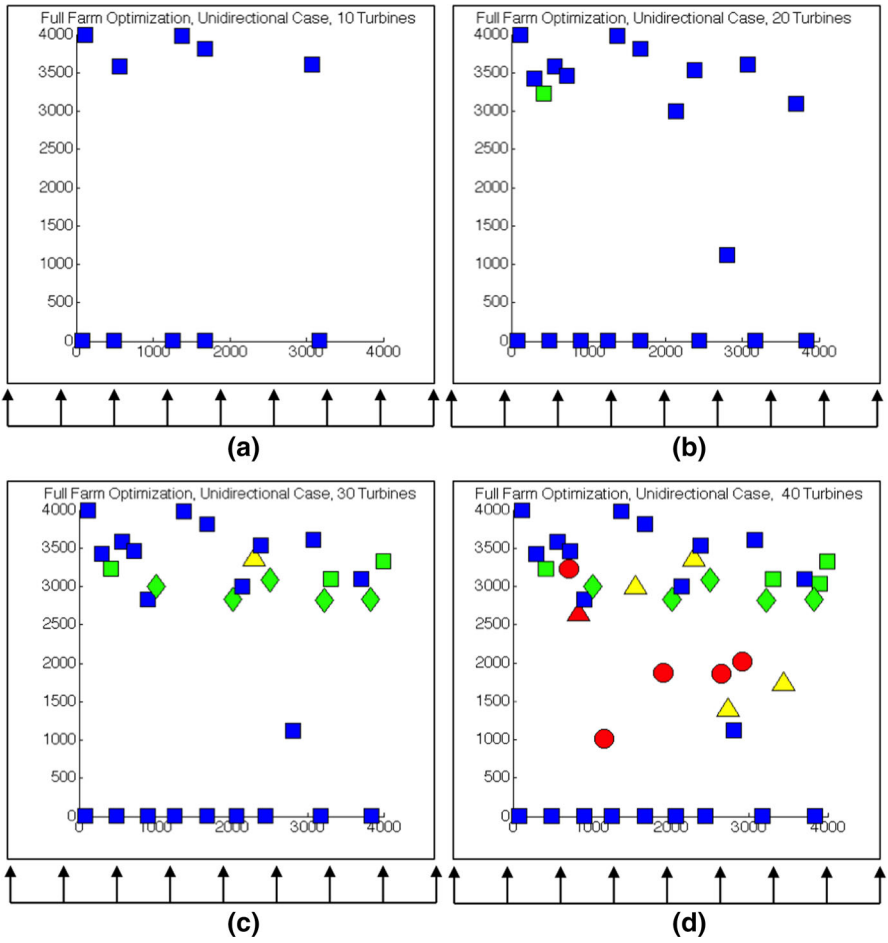

Fig. 11 Unidirectional case, full-farm hybrid EPS/GS, square field. **a** 10 Turbines (sub-farm 1), **b** 20 Turbines (sub-farm 2), **c** 30 Turbines (sub-farm 3), and **d** 40 Turbines (full farm)

Table 2 Unidirectional full-farm hybrid EPs/GA results, rectangular field

N	Objective	Power (MW)	Avg. hub height (m)	Avg. rotor radius (m)
40	−1.04E+08	175	117.62	58.20
30	−9.41E+07	163	134.47	66.51
20	−6.93E+07	110	134.84	66.91
10	−3.20E+07	55	134.84	66.91

developer would start by installing the first stage depicted in Fig. 6, and build adjacent stages as capital becomes available. The numerical results for each square sub-farm are compiled in Table 3 with the square full layout given in Fig. 13. The

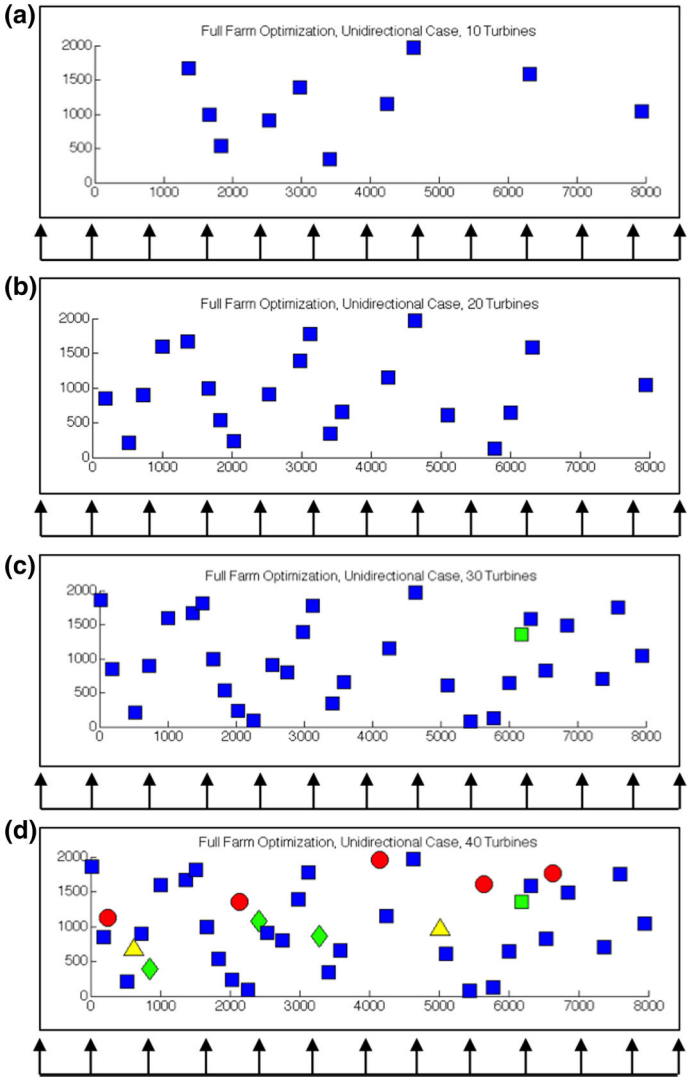

Fig. 12 Unidirectional Case, Full-Farm Hybrid EPS/GS, Rectangular Field. **a** 10 Turbines (sub-farm 1), **b** 20 Turbines (sub-farm 2), **c** 30 Turbines (sub-farm 3), and **d** 40 Turbines (full farm)

numerical results for the rectangular field are given in Table 4, with the rectangular full layout given in Fig. 14. Note that in both Tables 3 and 4, the objective evaluation is provided only for the full farm (40 turbines), as this is the objective determined by the EPS for the completed farm. Sub-farms (30, 20, and 10 turbines) are created by removing turbines one at a time from the completed farm using the GA, so the objective is not directly calculated for each of the sub-farms.

Table 3 Unidirectional weighted multi-objective EPS results, square layout

N	Objective	Power (MW)	Avg. hub height (m)	Avg. rotor radius (m)
40	−9.15E+07	146	106.60	50.68
30		113	109.30	52.09
20		82.0	112.98	55.17
10		36.7	107.91	51.75

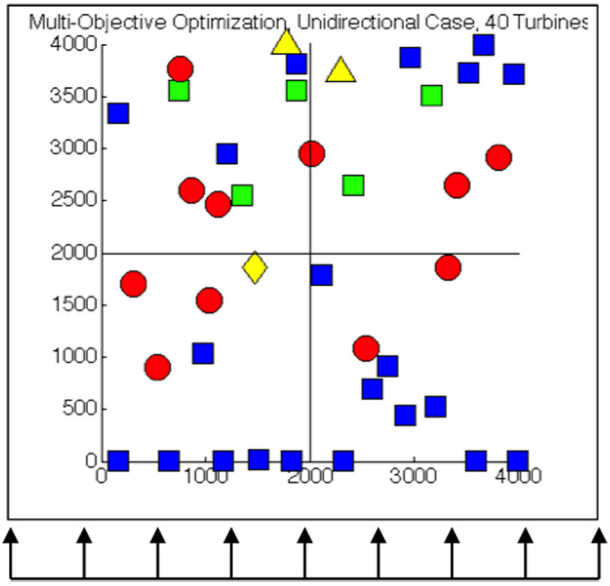

Fig. 13 Unidirectional case, multi-objective EPS, square field, 40 turbines

Table 4 Unidirectional weighted multi-objective EPS results, square layout

N	Objective	Power (MW)	Avg. hub height (m)	Avg. rotor radius (m)
40	−6.31E+07	167	117.83	57.69
30		133	120.27	58.62
20		90.3	119.02	57.48
10		45.1	121.91	58.91

6.2 Multidirectional case

6.2.1 Full-farm optimization with hybrid EPS/GA, multidirectional case

The multidirectional full-farm optimization square results are reported in Table 5, with the respective square layouts given in Figure 15.

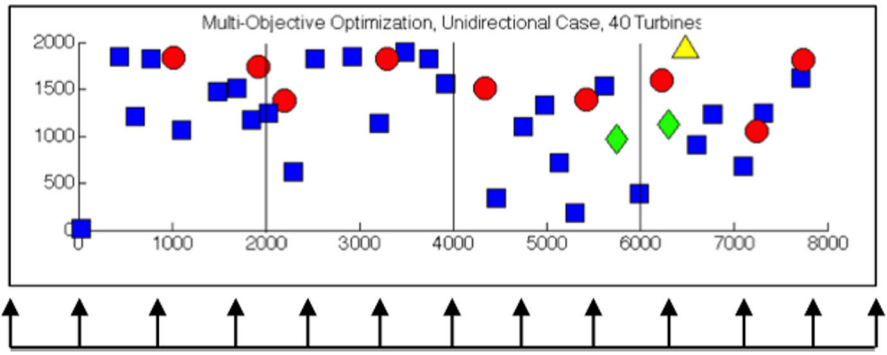

Fig. 14 Unidirectional case, multi-objective EPS, rectangular field, 40 turbines

Table 5 Multidirectional full-farm hybrid EPs/GA results, square field

N	Objective	Power (MW)	Avg. hub height (m)	Avg. rotor radius (m)
40	−1.54E+08	126	100.32	49.91
30	−7.91E+07	105	101.61	50.54
20	−7.59E+07	77.5	105.63	52.61
10	−4.32E+07	40.9	107.98	53.82

The multidirectional full-farm optimization rectangular results are reported in Table 6, with the respective rectangular layouts given in Figure 16.

6.2.2 *Weighted multi-objective EPS over sequential, adjacent land, multidirectional case*

The multidirectional multi-objective optimization square results are reported in Table 7, with the square layout given in Fig. 17. The multidirectional multi-objective optimization rectangular results are reported in Table 8, with the rectangular layout given in Fig. 18. Note that in both Tables 7 and 8, the objective evaluation is provided only for the full farm (40 turbines), as this is the objective determined by the EPS for the completed farm. Sub-farms (30, 20, and 10 turbines) are created by removing turbines one at a time from the completed farm using the GA, so the objective is not directly calculated for each of the sub-farms.

7 Concluding discussion

The purpose of this work was to develop and explore a potential application of a multi-objective EPS and a novel hybrid EPS/GA algorithm. While a traditional EPS has been previously applied to wind farm optimization, these new algorithms have enabled approaching a significant challenge in this area, in that large onshore wind farms are installed in stages, requiring advanced optimization methods. To test the efficacy of these algorithms, we wanted to explore two prevalent means of real-

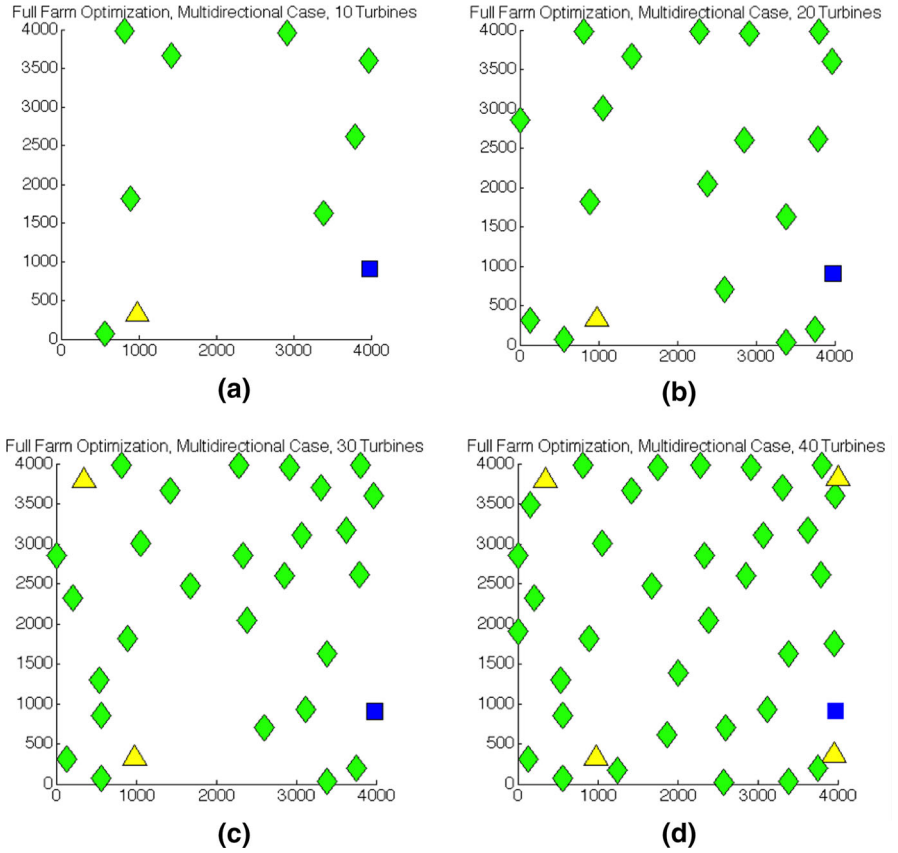

Fig. 15 Multidirectional case, full-farm hybrid EPS/GS, square field. **a** 10 Turbines (sub-farm 1), **b** 20 Turbines (sub-farm 2), **c** 30 Turbines (sub-farm 3), and **c** 40 Turbines (full farm)

Table 6 Multidirectional full-farm hybrid EPs/GA results, rectangular field

N	Objective	Power (MW)	Avg. hub height (m)	Avg. rotor radius (m)
40	−1.84E+08	161	111.55	55.62
30	−1.11E+08	127	109.81	54.74
20	−6.99E+07	82.8	109.74	54.67
10	−4.26E+07	45.2	113.82	56.80

world multi-stage wind farm layouts: (a) straight lines of turbines perpendicular to a predominant wind direction, with a significant downstream distance between subsequent rows, and (b) the use of new, adjacent land to build subsequent sub-farms.

The first method employed, the full-farm hybrid EPS/GA Algorithm, used an EPS to complete the optimization of turbine layout and geometry for a large

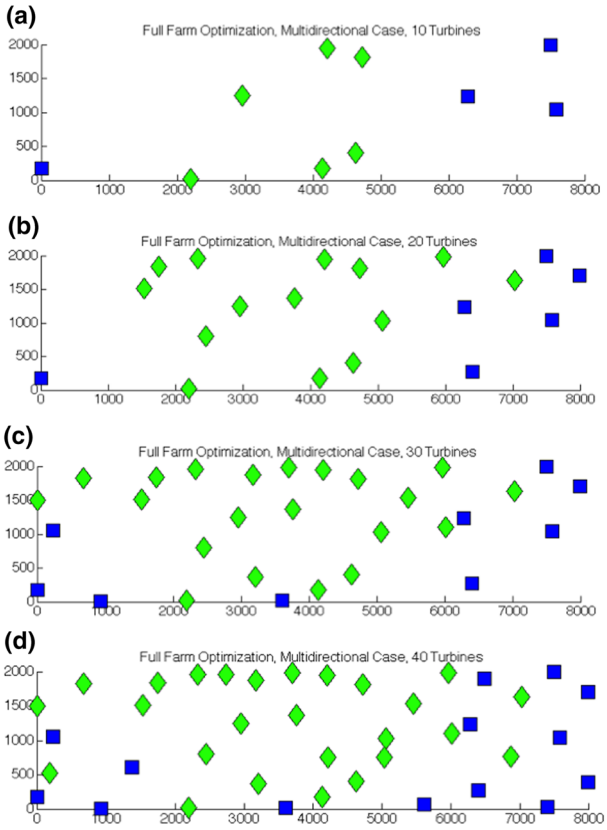

Fig. 16 Multidirectional case, full-farm hybrid EPS/GS, rectangular field. **a** 10 Turbines (sub-farm 1), **a** 20 Turbines (sub-farm 2), **a** 30 Turbines (sub-farm 3), and **a** 40 Turbines (full farm)

Table 7 Multidirectional weighted multi-objective EPS results, square layout

N	Objective	Power (MW)	Avg.hub height (m)	Avg. rotor radius (m)
40	−8.78E+08	217.83	134.81	66.90
30			134.84	66.91
20			134.84	66.91
10			134.84	66.91

completed farm, and a GA to systematically chose which turbines would be included in each stage prior to the completion of the full farm. This problem formulation has both a computationally expensive objective evaluation (due to the inclusion of advanced modeling) and a large solution search tree. The runtime for the EPS was comparable to that of previous wind farm optimization studies using advanced modeling [8], and the GA was run ten times using 100 parent strings, converging to the same result every time for both the uni- and multi-directional

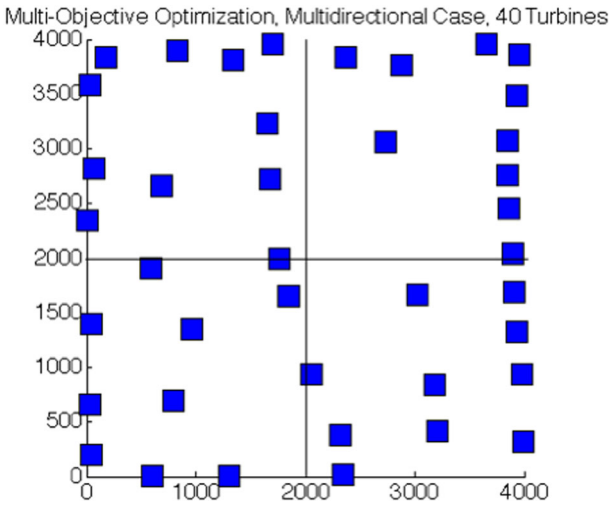

Fig. 17 Multidirectional case, multi-objective EPS, square field, 40 turbines

Table 8 Multidirectional weighted multi-objective EPS results, rectangular layout

N	Objective	Power (MW)	Avg. hub height (m)	Avg. rotor radius (m)
40	−9.08E+08	224.34	134.84	66.91
30			134.84	66.91
20			134.84	66.91
10			134.84	66.91

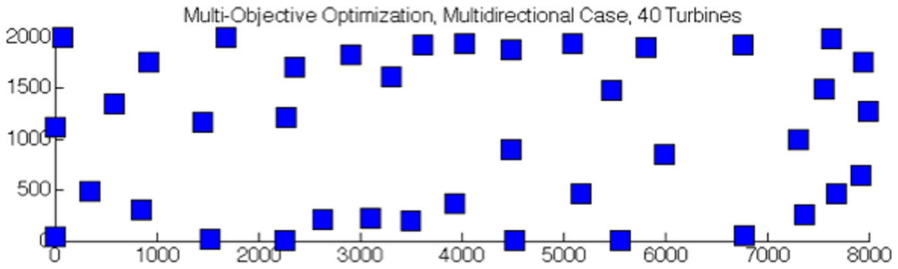

Fig. 18 Multidirectional case, multi-Objective EPS, rectangular field, 40 turbines

cases. The results of the hybrid EPS/GA as applied to multi-stage wind farm optimization were particularly interesting in a few ways. First, though many existing multi-stage farms are reminiscent of the rectangular layout presented here, the square layout was able to achieve a better objective evaluation (indicating a higher modeled profit) than the rectangular layout. The rectangular layout developed more power, however, which lends credibility to the prevalence of multi-stage farms

being oriented in this way for predominantly unidirectional wind. For both the square and rectangular cases, the turbines that were performing the least optimally—either having smaller geometries that don't generate as much power, or were upstream of many other turbines—were generally removed from the layouts first and saved for inclusion until the last stage. Both the unidirectional and multidirectional square cases, the first sub-farm—including only the first stage of ten turbines (Figs. 12a and 16a), exhibit "hollowed-out" behavior that has been evident in previous literature [7]. That is, the turbines attempt to maximize the downstream distance between them. For the unidirectional case, this corresponds to turbines moving toward the very front and back of the field; and for the multidirectional case, migration toward the outer edges of the field. The 10-turbine sub-farm results for the unidirectional square case is interesting to note, due to the fact that the resulting layout is two essentially straight lines of turbines across the front and back of the field. This result is commonly seen on some larger wind farms, like the aforementioned Horse Hollow Wind Energy Center in Texas—multiple straight lines of turbines that are oriented perpendicular to the prevailing oncoming wind direction. This layout suggests that this turbine placement method is potentially acceptable given there is significant downstream distance (in this case, 4km) for the wind speed within the wake to recover.

The second method, the weighted multi-objective EPS, explores the capability of the EPS when being applied to multiple layout fields at once. For the multi-stage wind farm application, this behavior mimics the addition of stages on adjacent plots of land. Based on the plots identified in Figs. 6, 10 turbines are placed in each of four stages to create 3 sub-farms and one complete farm. In this case, the square field also had a better objective evaluation than the rectangular field, though within this formulation it is much more significant. The rectangular field, however, included slightly larger turbines and generated more power. Again, there is clustering at the front and back of the square field for the unidirectional case, while the rectangular field saw clustering only near the back. This suggests that for the same square kilometer area (1600km) and a predominant wind direction, the square field should be able to generate more profit over the life of the farm. This is particularly interesting to note considering these multi-objective optimized layouts used discrete, adjacent stages, which is commonly seen in real-world multi-stage wind farm layouts. For the multidirectional case, both the square layout and rectangular layout consisted of turbines that had selected the largest geometry possible given the defined size constraints. This indicates that the additional cost needed to purchase, install, and service these larger turbines is offset by their higher power development, leading to an increase in profit.

In conclusion, two methods are presented that are ideal for solving the multi-stage wind farm optimization problem, a multi-objective EPS algorithm and a hybrid EPS/GA. The hybrid EPS/GA, which is specifically designed to accommodate problems that require both a continuous solutions space and include a large search tree, showed promise as applied to the current problem, and could potentially be applied to other large system optimization problems, such as the layout of wave energy conversion devices (a similar problem formulation to wind farms), or the location of generators in a large power network. While neither the EPS or the EPS/

GA have guaranteed global optimality, each of these algorithms was executed ten times, and the most optimal result was chosen for inclusion in this work. It therefore pertinent to explore turbine movement patterns and layout features that are common across results, as opposed to suggesting any one layout is indeed globally optimal. Additionally, there are a few insights gained from solving this multi-stage wind farm optimization that can be translated to new wind farm development. For a multi-stage farm, the multi-objective optimization presented here was able to develop a layout with significantly higher profit than the full-farm optimization (for the more real-world applicable multidirectional case). This suggests that while the optimization of the full farm is vital, the performance of each sub-farm leading to the final farm's completion must also be strongly considered. This effect is less clear for a farm with a single, predominant wind direction. Additionally, the effect of enabling turbines to capitalize on a greater wind resource at higher altitudes (evidenced by the selection of larger turbine geometries) and greater wind speeds within wakes (evidenced by maximizing the downstream distance between turbines) is clearly noted for each of the multi-stage examples, implying the importance of employing these capability in real world multi-stage farm development. Though these approaches to multi-stage wind farm development are novel and lack previous research against which to compare these results, this work may serve as a vital first step toward bettering not only our understanding of how to build large onshore wind farms, but how to use multiple heuristic optimization methods in tandem to capitalize on the best attributes of each.

References

Abramson M, Audet C, Couture G, Dennis Jr J, Le Digabel S, Tribes C (2009) NOMAD: a blackbox optimization solver. https://gerad.ca/nomad/Project/Home.html

Audet C, Dennis JE (2006) Mesh adaptive direct search algorithms for constrained optimization. SIAM J Optim 17(1):188–217. doi:10.1137/060671267

Audet C, Custódio AL, Dennis JE (2008a) Erratum: mesh adaptive direct search algorithms for constrained optimization. SIAM J Optim 18(4):1501–1503. doi:10.1137/060671267

Audet C, Savard G, Zghal W (2008b) Multiobjective optimization through a series of single-objective formulations. SIAM J Optim 19(1):188. doi:10.1137/060677513

Aytun Ozturk U, Norman BA (2004) Heuristic methods for wind energy conversion system positioning. Electric Power Syst Res 70(3): 179–185, doi: 10.1016/j.epsr.2003.12.006, http://linkinghub.elsevier.com/retrieve/pii/S0378779603003043

Benatiallah A, Dakyo B (2010) Modelling and optimisation of wind energy systems. Jordan J Mech Indust Eng 4(1):143–150

Bilbao M, Alba E (2009) Simulated annealing for optimization of wind farm annual profit. In: 2009 2nd international symposium on logistics and industrial informatics,Ieee, Linz, Australia, 2, pp 1–5, doi: 10.1109/LINDI.2009.5258656, http://ieeexplore.ieee.org/lpdocs/epic03/wrapper.htm?arnumber=5258656

Cagan J, Shimada K, Yin S (2000) A survey of computational approaches to three- dimensional layout problems. Comput Aided Des 412:1–33

Chen L, Macdonald E (2011) A new model for wind farm layout optimization with landowner decisions. In: ASME International Design Engineering Technical Conference, pp 1–12

Chowdhury S, Messac A, Zhang J, Castillo L, Lebron J (2010) Optimizing the unrestricted placement of turbines of differing rotor diameters in a wind farm for maximum power generation. ASME IDETC, Montreal

Chowdhury S, Zhang J, Messac A, Castillo L (2013) Optimizing the arrangement and the selection of turbines for wind farms subject to varying wind conditions. Renew Energy 52: 273–282, doi: 10.1016/j.renene.2012.10.017, http://linkinghub.elsevier.com/retrieve/pii/S0960148112006544

Conn AR, Scheinberg K, Vicente LN (2008) Introduction to Derivative-free optimization. MOS-SIAM Series on Optimization, Philadelphia, PA

Di Pillo G, Fasano G, Liuzzi G, Lucidi S, Piccialli V, Rinaldi F, Sciandrone M (2015) DFL - Derivative-Free Library. http://www.dis.uniroma1.it/lucidi/DFL/

DuPont B, Cagan J (2013) Multi-stage optimization of wind farms with limiting factors. ASME International Design Engineering Technical Conferences/Computers in Engineering, Portland, OR

DuPont B, Cagan J, Moriarty P (2016) An Advanced Modeling System for Optimization of Wind Farm Layout and Wind Turbine Sizing Using a Multi-Level Extended Pattern Search Algorithm. Energy (Accepted, In Press)

DuPont BL, Cagan J (2010) An extended pattern search approach to wind farm layout optimization. ASME IDETC, Montreal, pp 1–10

DuPont BL, Cagan J (2012) An extended pattern search approach to wind farm layout optimization. ASME J Mech Des 134:1–18. doi:10.1115/1.4006997

DuPont BL, Cagan J, Moriarty P (2012) Optimization of wind farm layout and wind turbine geometry using a multi-level extended pattern search algorithm that accounts for variation in wind shear profile shape. In: ASME IDETC, Chicago, IL

Elkinton C, Manwell J, McGowan J (2005) Offshore wind farm layout optimization (OWFLO) project: an introduction. optimization

Elkinton C, Manwell J, McGowan J (2006) Offshore wind farm layout optimization (OWFLO) project: Preliminary results. American Institute of Aeronautics and Astronautics pp 1–9, http://arc.aiaa.org/doi/pdf/10.2514/6.2006-998

Emami A, Noghreh P (2010) New approach on optimization in placement of wind turbines within wind farm by genetic algorithms. Renewable Energy 35(7): 1559–1564, doi: 10.1016/j.renene.2009.11.026, http://linkinghub.elsevier.com/retrieve/pii/S0960148109005023

EON Climate and Renewables (2015) Roscoe wind energy complex. Technical report

Fingersh L, Hand M, Laxson A (2006) Wind turbine design cost and scaling model. Technical Report, December, National Renewable energy Laboratory, Golden CO

Fowler KR, Reese JP, Kees CE, Dennis JE, Kelley CT, Miller CT, Audet C, Booker AJ, Couture G, Darwin RW, Farthing MV, Finkel DE, Gablonsky JM, Gray G, Kolda TG (2008) Comparison of derivative-free optimization methods for groundwater supply and hydraulic capture community problems. Adv Water Resour 31(5):743–757. doi:10.1016/j.advwatres.2008.01.010

Grady S, Hussaini M, Abdullah M (2005) Placement of wind turbines using genetic algorithms. Renew Energy 30(2): 259–270, doi: 10.1016/j.renene.2004.05.007, http://linkinghub.elsevier.com/retrieve/pii/S0960148104001867

Hooke R, Ta Jeeves (1961) "Direct Search" solution of numerical and statistical problems. J ACM 8(2):212–229. doi:10.1145/321062.321069

Huang H (2009) Efficient hybrid distributed genetic algorithms for wind turbine positioning in large wind farms. In: proceedings of the 2009 IEEE International Symposium on Industrial Electronics (ISIE), pp 2196–2201, doi: 10.1109/ISIE.2009.5213603, http://ieeexplore.ieee.org/lpdocs/epic03/wrapper.htm?arnumber=5213603

Huang HS (2007) Distributed genetic algorithm for optimization of wind farm annual profits. In: proceedings of the 2007 International Conference on Intelligent Systems Applications to Power Systems pp 1–6, doi: 10.1109/ISAP.2007.4441654, http://ieeexplore.ieee.org/lpdocs/epic03/wrapper.htm?arnumber=4441654

Jensen N (1983) A note on wind generator interaction. Technical report, Riso National Laboratory, Roskilde

Katic I, Hojstrup J, Jensen N (1986) A simple model for cluster efficiency. European wind energy association conference and exhibition. Rome, pp 407–410

Kelley N, Shirazi M, Jager D, Wilde S, Adams J, Buhl M, Sullivan P, Patton E (2004) Lamar low-level jet project interim report. Technical Report, January, National Renewable Energy Laboratory, Golden CO

Kusiak A, Zheng H (2010) Optimization of wind turbine energy and power factor with an evolutionary computation algorithm. Energy 35(3):1324–1332. doi:10.1016/j.energy.2009.11.015

Le Digabel S (2011) Algorithm 909: NOMAD: Nonlinear Optimization with the MADS Algorithm. ACM Trans Math Softw 37(4):44:1–44:15, doi: 10.1145/1916461.1916468, http://portal.acm.org/citation.cfm?doid=1916461.1916468

Manwell J, McGowan J, Rogers A (2009) Wind energy explained: theory, design and application, 2nd edn. John Wiley and Sons, Chichester

Messac A (1996) Physical programming: effective optimization for computational design. AIAA J 34(1):149–158

Mosetti G, Poloni C, Diviacco B (1994) Optimization of wind turbine positioning in large windfarms by means of a genetic algorithm. J Wind Eng Indust Aerodyn 51(1): 105–116, doi: 10.1016/0167-6105(94)90080-9, http://linkinghub.elsevier.com/retrieve/pii/0167610594900809

Mustakerov I, Borissova D (2010) Wind turbines type and number choice using combinatorial optimization. Renew Energy 35(9): 1887–1894, doi: 10.1016/j.renene.2009.12.012, http://linkinghub.elsevier.com/retrieve/pii/S0960148109005618

Next Era Energy Resources (2006) Horse Hollow I, II & III Wind Energy Center. Technical report, http://www.nexteraenergyresources.com/content/where/portfolio/pdf/horsehollow.pdf

NREL (2010) NREL JEDI Models. http://www.nrel.gov/analysis/jedi/download.html

Oregon DOE (2010) Stateline Wind Project. Technical report, http://www.oregon.gov/ENERGY/SITING/Pages/SWP.aspx

Rasuo B, Bengin A (2010) Optimization of wind farm layout. FME Trans 38:107–114

Salcedo-Sanz S, Gallo-Marazuela D, Pastor-Sánchez a, Carro-Calvo L, Portilla-Figueras a, Prieto L (2014) Offshore wind farm design with the Coral Reefs Optimization algorithm. Renew Energy 63: 109–115, doi: 10.1016/j.renene.2013.09.004, http://linkinghub.elsevier.com/retrieve/pii/S0960148113004710

Samorani M (2010) The wind farm layout optimization problem the wind farm layout optimization problem. Technical report

Senecal PK (2000) Numerical optimization using the Gen4 Micro-Genetric Algorithm Code. PhD thesis, University of Wisconsin-Madison

Sisbot S, Turgut O, Tunc M, Camdali U (2009) Optimal positioning of wind turbines on gokceada using multi-objective genetic algorithm. Wind Energy 13(4):297–306. doi:10.1002/we

Terra-Gen Power L (2015) Alta Wind Energy Center. Technical report

Torczon V (1997) On the convergence of pattern search algorithms. SIAM J Optim 7(1): 1–25, doi: 10.1137/S1052623493250780, http://epubs.siam.org/doi/abs/10.1137/S1052623493250780

Vaz AIF, Vicente L (2007) A particle swarm pattern search method for bound constrained nonlinear optimization. J Glob Optim 39(2):1–27

Wan C, Wang J, Yang G, Li X, Zhang X (2009) Optimal micro-siting of wind turbines by genetic algorithms based on improved wind and turbine models. In: Proceedings of the 48h IEEE Conference on Decision and Control (CDC) held jointly with 2009 28th Chinese Control Conference (3), pp 5092–5096, doi: 10.1109/CDC.2009.5399571, http://ieeexplore.ieee.org/lpdocs/epic03/wrapper.htm?arnumber=5399571

Wan C, Wang J, Yang G, Zhang X (2010) Optimal micro-siting of wind farms by particle swarm optimization. ICSI 2010:198–205

Wang F, Liu D, Zeng L (2009a) Modeling and simulation of optimal wind turbine configurations in wind farms. In: 2009 World Non-Grid-Connected Wind Power and Energy Conference pp 1–5, doi: 10.1109/WNWEC.2009.5335756, http://ieeexplore.ieee.org/lpdocs/epic03/wrapper.htm?arnumber=5335756

Wang F, Liu D, Zeng L (2009b) Study on computational grids in placement of wind turbines using genetic algorithm. 2009 World Non-Grid-Connected Wind Power and Energy Conference 2, pp 1–4, doi: 10.1109/WNWEC.2009.5335776, http://ieeexplore.ieee.org/lpdocs/epic03/wrapper.htm?arnumber=5335776

Wilson D, Cussat-Blanc S, Veeramachaneni K, O'Reilly UM, Luga H (2014) A continuous developmental model for wind farm layout optimization. Proceedings of the 2014 conference on Genetic and evolutionary computation - GECCO '14 pp 745–752, doi: 10.1145/2576768.2598383, http://dl.acm.org/citation.cfm?doid=2576768.2598383

Yin S, Cagan J (2000) An extended pattern search algorithm for three-dimensional component layout. ASME J Mech Des 122:102–108

Zhang J, Chowdhury S, Messac A, Castillo L, Lebron J (2010) Response surface based cost model for onshore wind farms using extended radial basis functions. ASME Internation Design Engineering Technical Conference. Montreal, QC, Canada, pp 1–16